Characterization and Application of Nanomaterials (2022) Volume 5 Issue 2
doi:10.24294/can.v5i2.1684

ORIGINAL RESEARCH ARTICLE

Effect of an oscillating magnetic field in polymeric columns with magnetic nanoparticles

Violeta Maricela Dalgo Flores*, Gabriela Cristina Chango Lescano, John Germán Vera Luzuriaga

Escuela Superior Politécnica de Chimborazo, Riobamba 060155, Ecuador. E-mail: violeta.dalgo@espoch.edu.ec

ABSTRACT

Magnetite magnetic nanoparticles (MNP) exhibit superparamagnetic behavior, which gives them important properties such as low coercive field, easy superficial modification and acceptable magnetization levels. This makes them useful in separation techniques. However, few studies have experimented with the interactions of MNP with magnetic fields. Therefore, the aim of this research was to study the influence of an oscillating magnetic field (OMF) on polymeric monolithic columns with vinylated magnetic nanoparticles (VMNP) for capillary liquid chromatography (cLC). For this purpose, MNP were synthesized by coprecipitation of iron salts. The preparation of polymeric monolithic columns was performed by copolymerization and aggregation of VMNP. Taking advantage of the magnetic properties of MNP, the influence of parameters such as resonance frequency, intensity and exposure time of a OMF applied to the synthesized columns was studied. As a result, a better separation of a sample according to the measured parameters was obtained, so that a column resolution (R_s) of 1.35 was achieved. The morphological properties of the columns were evaluated by scanning electron microscopy (SEM). The results of the chromatographic properties revealed that the best separation of the alkylbenzenes sample occurs under conditions of 5.5 kHz and 10 min of exposure in the OMF. This study constitutes a first application in chromatographic separation techniques for future research in nanotechnology.

Keywords: Capillary Liquid Chromatography; Oscillation Frequency; Nanoparticles; Superparamagnetic

ARTICLE INFO

Received: 14 May 2022
Accepted: 13 July 2022
Available online: 27 July 2022

1. Introduction

Capillary liquid chromatography (cLC) is one of the most widely used analytical techniques for the qualitative and quantitative analysis of numerous chemical compounds. For this reason, the development of cLC columns has evolved significantly. Among the great diversity of columns, monolithic columns stand out because they allow working at high flow rates, therefore, obtaining fast separations without the use of high pressures in the system[1,2]. In addition, the bed is anchored directly to the support wall, so the use of retention fry is not necessary. These columns have been widely used to separate individual components of various samples[3,4].

There are two types of monolithic columns: polymers, which consist of obtaining organic polymers by in-situ polymerization of an organic or hydro-organic mixture, and silicon-based monolithic prepared by sol-gel processes[5,6]. Polymer monomers have some advantages over silica, such as fast and simple preparation, versatility of polymer functionalization and improved chemical stability over a wide pH range (2–12)[7]. These monoliths are widely used in the analysis of proteins, high molecular weight molecules and small molecules in food, environmental and pharmaceutical fields[8–11].

Therefore, the latter type of monoliths was selected for this study. However, despite the advantages of polymer monolithic columns, it should be noted that their limitation lies in the low surface area values (<10 m/g) compared to silica columns. To solve this drawback, in recent years, various nano-materials have been incorporated into these stationary phases. Thus, for example, glycidyl methacrylate (GMA) monoliths are described which functionalized with various types of Au, Ag and Ni-Co metal nanoparticles resulting in a manipulation in the retention of proteins and other small molecules[12,13].

As nanotechnology advances, new nanomaterials are destined to emerge as powerful materials that enable analytical determinations with improved sensitivity. The most commonly used in separation techniques include: silica and carbon nanoparticles (NP) (mainly fullerenes and carbon nanotubes) and metallic (iron oxide, gold, silver and europium)[14]. Applications of these NPs include their use as adsorbents in solid-phase extraction and microextraction[5,12], as well as the development of stationary phases incorporating these nanostructured materials. For example, recently, vinylated micro nanoparticles have been incorporated into the monolithic columns of GMA, which provided an increase in the surface area of the monoliths.

This in turn lead to an increase in the retention and effectiveness of the chromatographic column[15]. However, the incorporation of magnetic nanoparticles (MNP) into this type of stationary phases has been little studied[10,15]. Hence, the aim of the present investigation which seeks to take advantage of the superparamagnetic behavior of MNP in the efficiency of chromatographic separations.

The oscillating magnetic field (OMF) is one of the different types of magnetic fields, which is produced by alternating current electromagnets with a periodic change of intensity that depends on the frequency of the magnet and the type of wave. The OMF applied in the form of reverse polarity pulses can be homogeneous in the area enclosed by the magnetic field coil or heterogeneous where the intensity decreases as the distance from the center of the coil increases[16].

Applying the theory of electromagnetism and the laws of Biot-Savart, Ampère Ohm and Kirchhoff, the motion of particles affected by a OMF is obtained. The Biot-Savart law states that if the current I passes through the conducting wire, a magnetic field is generated[17]. To denote the presence of a magnetic field in a given region of space, one must work with the magnetic field strength H. This relation is linear in most materials (equation 1).

$$B = \mu H \quad (1)$$

Where: B is the magnetic flux density (Teslas) and μ the magnetic permeability of the material ($T*m*A^{-1}$). With this law, the relation of the magnetic field can be found for any point in space with current I[18]. On the other hand, Ampère's circulation law is represented by equation 2.

$$\oint \vec{B} \cdot d\vec{l} = \mu_0 I \quad (2)$$

Where: dl is the length differential of the curve; μo is the magnetic permeability in vacuum ($\mu_o = 4\pi*10^{-7}\ T*m*A^{-1}$).

The field lines of B are concentric circles lying in planes perpendicular to the axis of the wire, with center in it. If a region of space is available, then the number of field vectors, traversing a surface, gives the magnetic flux conditions. Applying the double integral, the flux is divided by a certain surface area S, and B is obtained, as shown in equation 3[19].

$$B = \frac{\Phi}{S} = \mu H \quad (3)$$

Where: Φ is the magnetic flux through an area S in scalar product with B, with Weber units.

If there is more than one magnetic field source, it will provide intensive movements of the NP in different directions and consequently improves mass transfer[20,21]. The magnetic field generates the movement of the MNP contained in the monolith of the polymeric column (**Figure 1**).

In the present investigation, the influence of a OMF on polymeric monolithic columns with vinylated magnetite magnetic nanoparticles (VMNP) for cLC was studied. For this purpose, polymeric monolithic columns were prepared by the copolymerization method with butyl methacrylate (BMA) and

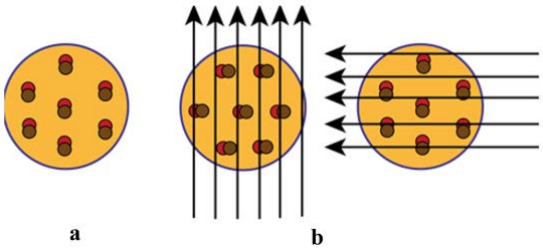

Figure 1. Movement of the MNP generated by a magnetic field: (**a**) position of the MNP in the absence of magmatic field and (**b**) displacement of the MNP according to the direction of the field line.

ethylene glycol dimethacrylate (EDMA) monomers by thermal initiation and subsequent aggregation of VMNP. Then, taking advantage of the magnetic properties of the MNP, the influence of various parameters (resonance frequency, intensity and exposure time) of a OMF applied on the synthesized columns was studied. The influence of these parameters on the morphological properties was evaluated by scanning electron microscopy (SEM). While, to monitor the effect on chromatographic properties, the separation of alkylbenzenes (ABS) samples in cLC in reverse elution mode was studied.

2. Materials and methods

2.1 Obtaining of polymeric monolithic columns

Monolithic columns were prepared using fused silica capillaries. The polyimide coating of 794 μm external diameter and 500 μm internal diameter, supplied by multi-micro technology (Phoenix, USA). In order to ensure covalent bonding with the monolith, the inner wall of the fused silica capillary was modified with 3-(trimethoxysilyl) propyl methacrylate (γ-MPS) from Sigma-Aldrich (Milwaukee, USA). For this purpose, the procedure described by Petro, Svec and Fréchet[22] was adopted.

The preparation of the polymerization mixtures was carried out in a glass cabinet, using an OHAUS model EX224 analytical balance (Mexico D.F., Mexico). The polymerization mixture was composed of BMA from Sigma-Aldrich (Milwaukee, USA) as functional monomer. EDMA from Sigma-Aldrich (Milwaukee, USA) and a ternary porogenic solvent, consisting of a mixture of 1,4-butanediol from Sigma-Aldrich (Milwaukee, USA), 1-propanol from Scharlau (Barcelona, Spain) and ultrapure water, obtained from a Nanopure II purification system from Barnstead (Boston, USA), were used as the binding agent. Azobisisobutyronitrile (AIBN) from Fluka (Buchs, Switzerland) was used as initiator of the polymerization reaction.

To the polymerization mixture, VMNP were added up to a final concentration of 2% by weight. The method selected to disperse the VMNP into the polymerization mixture was sonication, since it is the most recommended for the homogeneous distribution of nanomaterials in aqueous media. For this, once the mixture was prepared in a vial, it was agitated in a Heidolph vortex, model REAX 2000 (Schwabach, Germany), sonicated in a Bransonic ultrasonic bath model 2510R-MT (Boston, USA) for 15 min and purged with nitrogen, according to the method proposed by Carrasco, Ramis and Herrero[15]. **Table 1** shows the composition of the polymerization mixture studied.

Table 1. Composition of the polymerization mixture used

Components	Concentration (% weight)
Butyl methacrylate (BMA)	17.9
Ethylene glycol dimethacrylate (EDMA)	12.0
1,4-Butane diol	34.6
1-Propanol	28.2
Water(H_2O)	6.9
Azobisisobutyronitrile (AIBN)	0.4

The pretreated 10 cm long molten silica capillaries were capillary-filled entirely with the polymerization mixture and sealed at their ends. Thermal polymerization was carried out in a Pol-Eko-Aparatura model SRN 115 STD oven (Wodzislaw Sl¾ski, Poland) at 70 °C for 20 h. After the polymerization process was completed, methanol from VWR-Prolabo Chemicals (Paris, France) was passed through the obtained monolithic columns for 15 min in order to remove porogenic solvents and possible unreacted monomers, using a Shimadzu LC-10AS pump (Columbia, USA).

2.2 Synthesis and characterization of MNP

This section describes the synthesis and characterization of MNP with and without vinylation. The preparation of MNP was carried out by co-

precipitation, according to the procedure described by Yang *et al.*[23]. After the reaction was finished, the precipitate was collected with the help of a magnet; it was washed repeatedly with water and ethanol from VWR- Prolabo Chemicals (Paris, France) and the product was dried in an oven, at 60 °C for 12 h. To modify the surface of MNP with vinyl groups, 4 mL of γ-MPS reagent was added over 50 mg of MNPs; then, 1 mL of a 1:1 (v/v) water-ethanol mixture was added. The reaction was carried out under nitrogen atmosphere at a temperature of 40 °C for 12 h. Finally, the MNP was washed several times with ethanol and dried in the oven at 60 °C for 6 h.

The VMNP was characterized using a Jasco FTIR, model 4100 (Oklahoma, USA).

2.3 Preparation of the test sample

A sample of ABS consisting of toluene ethylbenzene propylbenzene and butyl benzene from Riedel de Haen (Hannover, Germany), was used as the analyte. The ABS stock solution was prepared from a concentration of 1,000 µg⁄mL in acetonitrile (MeCN) from VWR Prolabo Chemicals (Paris, France), and kept at −20 °C. From this, a 10 µg⁄mL test mixture of uracil (Sigma-Aldrich, Milwaukee, USA) and ABS was prepared.

2.4 Instrumental in the generation of the OMF

The OMF is generated and the MNP vibration of the monolithic column is caused using an electromagnet consisting of a coil of 500 coils of copper wire wound around a ferrite core and two pieces of iron forming a slot 5 mm wide and 9.5 cm long where the monolithic columns were placed.

The electric current supplied to generate the magnetic field came from an RS PRO model GFG-8255A function generator (Northants, England), connected to a Krohn-Hite model 7600/7602 broadband amplifier (Massachusetts, USA). Electrolytic capacitors were used to store the electric charges and modify the output frequency (**Table 2**).

Table 2. Capacitance of the capacitors used, resonance frequencies and magnetic flux densities obtained

Capacitor capacitance C(F)	Resonant frequency f_O (Hz)	Comment intensity 1(A)	Magnetic flux density B_g (mT)
4.7×10^{-3}	2	1.15	8.028
$l.0 \times 10^{-3}$	8	0.79	5.515
$l.0 \times 10^{-6}$	198	0.10	0.698
$l.0 \times 10^{-9}$	5,500	$2.l \times 10^{-6}$	$L.466 \times 10^{-5}$
$l.0 \times 10^{-12}$	228,000	Not measured	Not measured

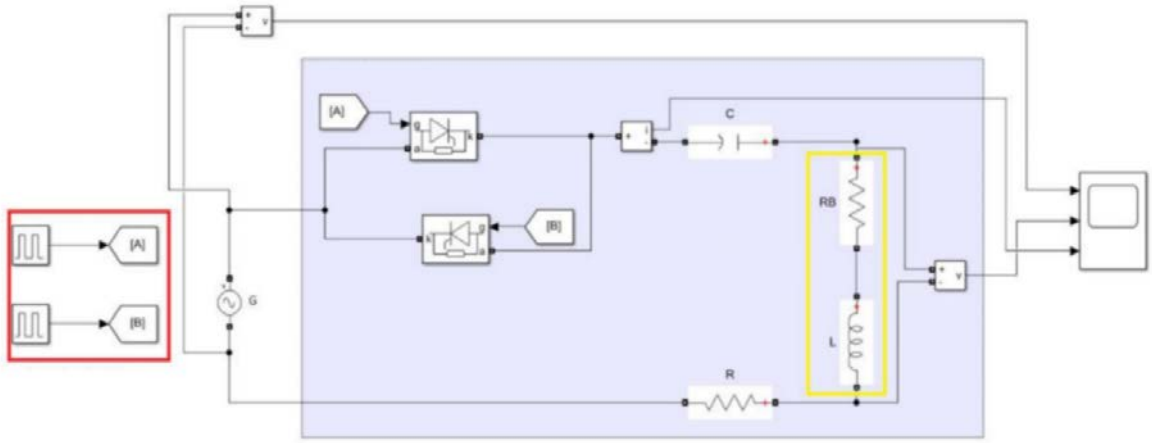

Figure 2. Circuit used in the generation of OMF.
Note: A and B: terminals; G: alternating current generator; C: variable capacitor; R: resistor; RB: coil resistance; L: inductor.

The current intensity was measured with a Fluke model 179 series multimeter. A Lab-Volt model AC 793G oscilloscope (New Jersey, USA) was connected to the system to obtain a graphical

representation of the electrical signals, their variation over time, and to monitor the signal voltage. **Figure 2** shows the circuit designed in Matlab with the above representation.

In **Table 3** the parameters and operating conditions of the OMF considered in the study of monolithic columns prepared using VMNP are given.

Table 3. OMF parameters and working conditions used in the study

Capacitors	**Capacity**	**4700 µF~1 pF**
Coil	Number of turns	500
	Resistance	14.6 Ω
Function generator	Output signal	Sine wave
	Frequency	2.3 Hz ~ 228 kHz
Amplifier	Amplitude	20 Vpp
	Type of electrical component	Alterna
	Amplitude	25 Vpp

2.5 Chromatographic conditions

Monolithic columns at 25 °C with VMNP were connected to the cLC equipment with Shimadzu UV-VIS detector model SCL-10A (Columbia, USA), and conditioned with the mobile phase until a stable baseline was observed, i.e., a mixture of MeCN:water (30:70 v/v) in isocratic elution at a flow rate of 0.15 mL/min. A mixture of ABS in concentration of 10 µg⁄mL was used as analyte with an injection volume of 2 µL and a spectrophotometric determination of 214 nm.

2.6 Characterization of polymeric monolithic columns

The morphological study of the monolithic materials was performed using the JEOL scanning electron microscope model JSM-IT100 (Tokyo, Japan). An important aspect here was the stability of the dispersion of VMNPs in the polymerization mixture and consequently their homogeneous distribution in the polymeric matrix. Therefore, it was decided to study the degree of dispersion of the VMNPs in the monolithic beds obtained thermally. For this purpose, mixtures containing 2% of VMNPs were placed in several vials polymerized thermally. Samples were then taken at different polymerization times. As a result of this procedure, images were obtained in the Zhunma optical microscope model XSZ 107BN-T (Ningbo, China) of monolithic beds with VMNP, taken at 5 and 60 min after polymerization.

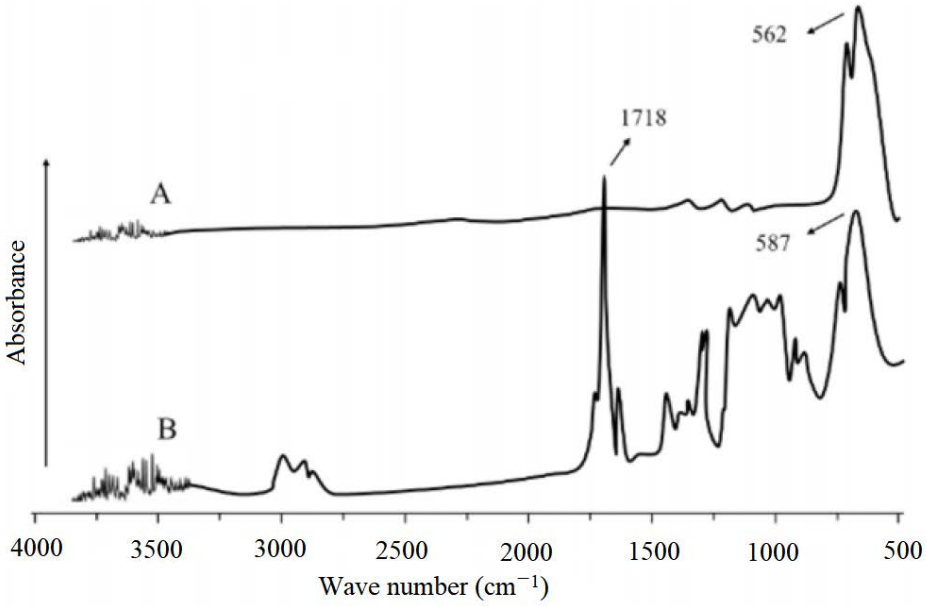

Figure 3. Infrared spectra of the surface of MNP: (**A**) unvinylated and (**B**) vinylated with γ-MPS.

3. Results and discussion

3.1 Characterization of vinylized MNP

Figure 3 shows the infrared spectra of unvinylated MNP (trace A) and VMNP (trace B). Both show an absorbance band at 562 cm^{-1}, corresponding to the Fe-O vibration of the magnetic core. In the VMNP (trace b) an intense band is observed at

1,718 cm^{-1} which is characteristic of the stress vibration of the γ-MPS ester carbonyl. The bands found at 1,633 and 3,004 cm^{-1} are due to the vibrations (stresses) of the C=C and C-H bonds of the γ-MPS compound.

The conditions for the preparation of the monoliths with VMNP were established considering a previous investigation[14]. The selected VMNP content was 2% in the polymerization mixture (**Table 1**). In the study, UV radiation was used as the polymerization initiation mode which can be performed in short times (15 min). This avoids possible sedimentation problems of the NPMV. However, in the present investigation, the capillaries used (internal diameter of 500 μm) are not transparent to UV radiation, so thermal initiation had to be resorted, which involved times of 20–24 h.

3.2 Characterization of monoliths with VMNP

In order to carry out the present characterization, the degree of dispersion of the NPMV in monolithic beds obtained by the thermal process was studied. The samples were taken at different polymerization times and observed by microscope. As a result, a random distribution of VMNP in the polymer matrix was determined, suggesting a homogeneous distribution of VMNPs. This can be explained by the rapid formation of polymerization nuclei (oligomers), which act as a support (host) for the VMNPs, thus preventing their sedimentation, properties mentioned in the work of Yu, Dave, Zhu, Quevedo and Pfeffer[24], investigated in depth by Ommen, Valverde and Pfeffer[25].

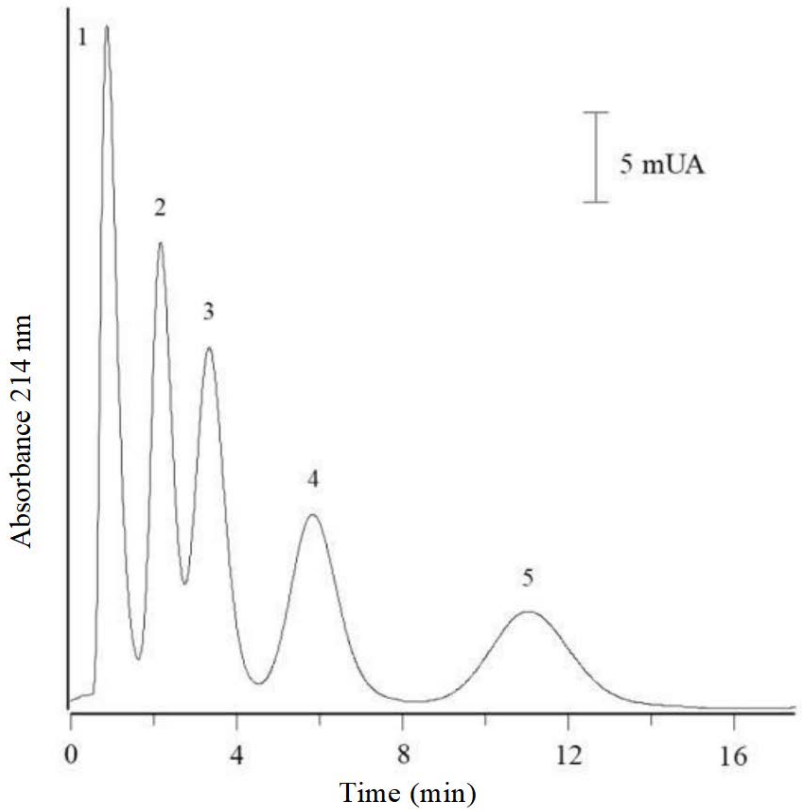

Figure 4. Separation of ABS using a monolithic polymeric column with 2% VMNP in the absence of magnetic field.
Note: Peaks: 1 uracil; 2 toluene; 3 ethylbenzene; 4 propylbenzene; 5 butylbenzene.

3.3 Chromatographic and morphological characterization of the monolith with VMNP

Figure 4 shows the separation of the ABS sample, using the monolithic column with VMNP content in the absence of OMF, according to the cLC working conditions previously indicated. These conditions presented the best separation results among several tests performed, in which parameters such as mobile phase composition and flow rate, injection volume and analyte concentra-

tion were measured.

In the chromatogram, a partial separation between the toluene and ethylbenzene pair was observed (peaks 2 and 3, respectively). It is intended to improve this separation by applying an external magnetic field to the monolithic columns with VMNP.

Figure 5 shows the morphology of the column, in which the microglobular structure characteristic of this type of polymers is observed. The existence of VMNP on the surface is not appreciated, since they are embedded (copolymerized) in the polymeric network, which was determined based on the study of the degree of dispersion of VMNP in the monolith.

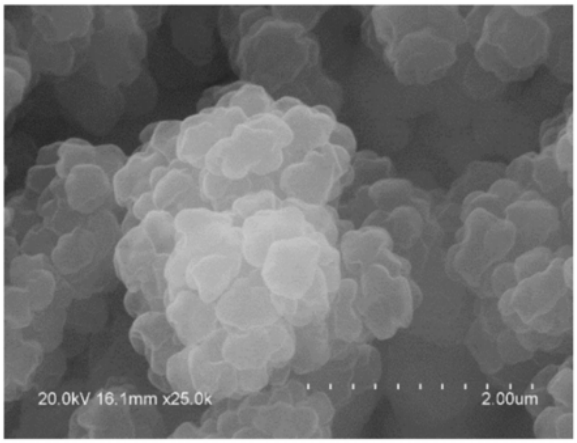

Figure 5. SEM image of the monolith with 2% VMNP, obtained at 20 kV and x25 k magnification.

3.4 Influence of time-constant OMF frequency variation

As discussed above magnetite NP is superparamagnetic so they are oriented and attracted by magnetic fields. For this reason, the influence of OMF application on the synthesized polymeric columns was studied. For this purpose, the columns were placed in the electromagnet gap and subjected to different magnetic fields at a fixed exposure time of 5 min. The magnetic field values produced in the air gap (B_g) were measured from different resonance frequencies (R), obtained from 2.3 Hz to 228 kHz for varying values of capacitors with capacities ranging from 4,700 μF to 1 pF.

The variation of the resonance frequency gives different maximum current intensity values. In turn, it will influence the magnetic flux density. According to Miranda, ferrites resonate at resonance frequencies when subjected to the action of a magnetic field, which influences chromatographic retention[26]. As this is a new study, the trend of better chromatographic separation as a function of column resolution has been seen, as presented in the results.

Figure 6 shows the separation of ABS at different resonance frequencies. As can be seen, as the OMF frequency increases, there is an increase in the retention time of the analytes, as described by Carrasco, Ramis and Herrero[15]. Also, it is observed that the resolution of all pairs of peaks improves, particularly, that of the toluene and ethylbenzene pair.

In order to evaluate the influence of OMF on the morphology of the studied monoliths, SEM tests were performed. However, in the overall image affected by different frequencies insignificant changes in microsphere size were observed compared to those obtained in the absence of OMF (**Figure 5**).

Although SEM images cannot show clear changes in the microgranule level, it is evident that the presence of superparamagnetic NP affects the monolith structure. This leads to an increase in the number of mesoscopic and micropores, which is closely related to the surface area and retention of analytes[15,27].

3.5 Influence of varying OMF exposure time at constant frequency

Continuing with the investigation, it was decided to study the influence of OMF exposure time at constant resonance frequency. For this purpose, the frequency of 5.5 kHz was chosen, which provided the best results in the previous section. In **Figure 7**, it is observed that an increase of the exposure time leads to an increase of the retention time of the analytes and to an improvement in the separation of the toluene-ethylbenzene pair up to 10 min. Values of time higher than this imply the decrease of the retention, accompanied by the loss of resolution of the toluene-ethylbenzene pair.

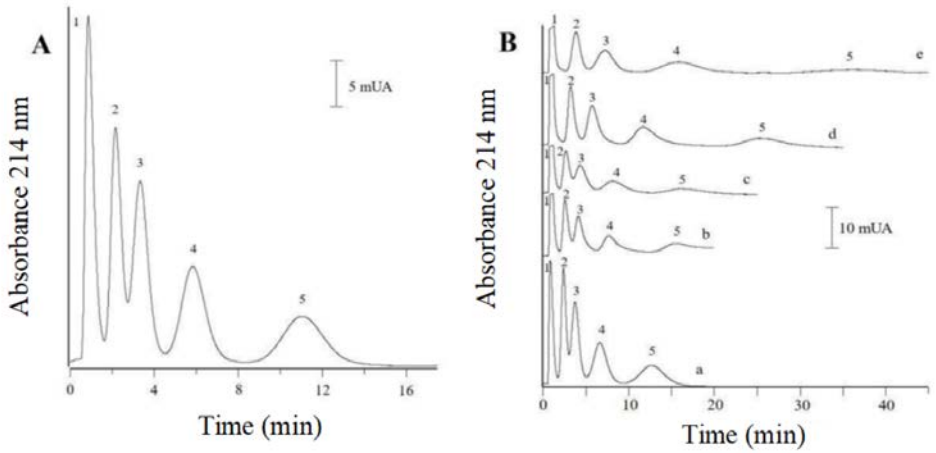

Figure 6. Separation of ABS sample using a polymeric monolithic column with 2% NPVM.
Note: (**A**) in the absence of OMF and (**B**) at different resonance frequencies: (a) 2 Hz, (b) 8 Hz, (c) 198 Hz, (d) 5.5 kHz and (e) 228 kHz.

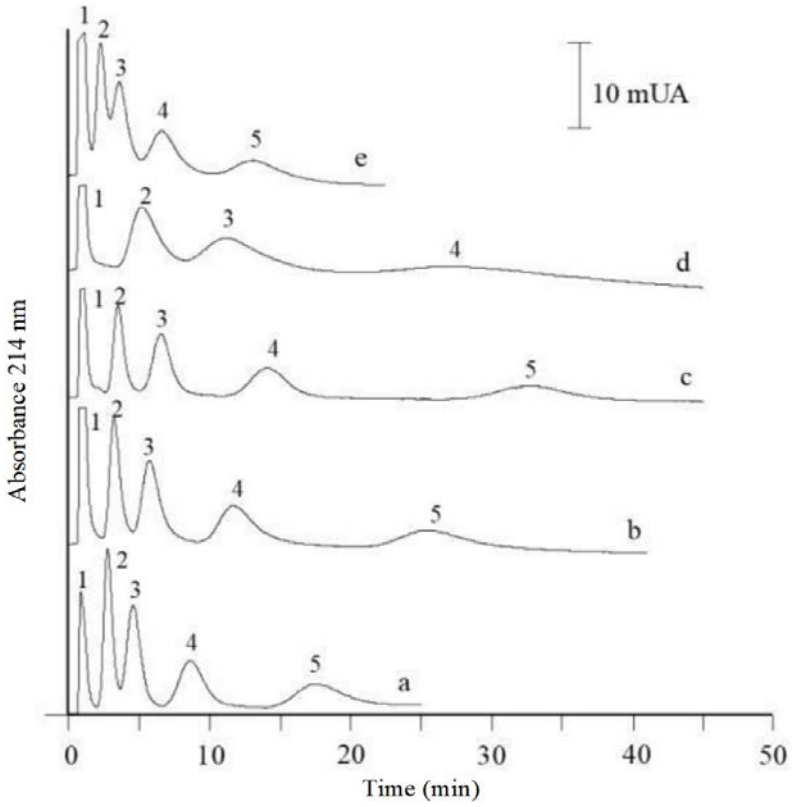

Figure 7. Separation of ABS using a monolithic polymeric column with 2% VMNP at constant resonance frequency (5.5 kHz) and different OMF generation times: (a) 1 min, (b) 5 min, (c) 10 min, (d) 20 min and (e) 60 min.

Table 4. Comparison of chromatographic resolution of ABS in the absence or presence of OMF

	Absence of OMF	**OMF* frequency variation**	**Time variation of OMF** exposure**
Peaks	Resolution R_s (n = 4)	Resolution R_s (n = 4)	Resolution R_s (n = 4)
Uracil-toluene	1.03	1.13	1.45
Toluene-ethylbenzene	1.02	1.27	1.35
Ethylbenzene-propylbenzene	1.12	1.78	1.86
Propylbenzene-butylbenzene	1.74	2.32	2.40

Note: * Results obtained at 5.5 kHz; ** Results obtained at 5.5 kHz and 10 min exposure to OMF.

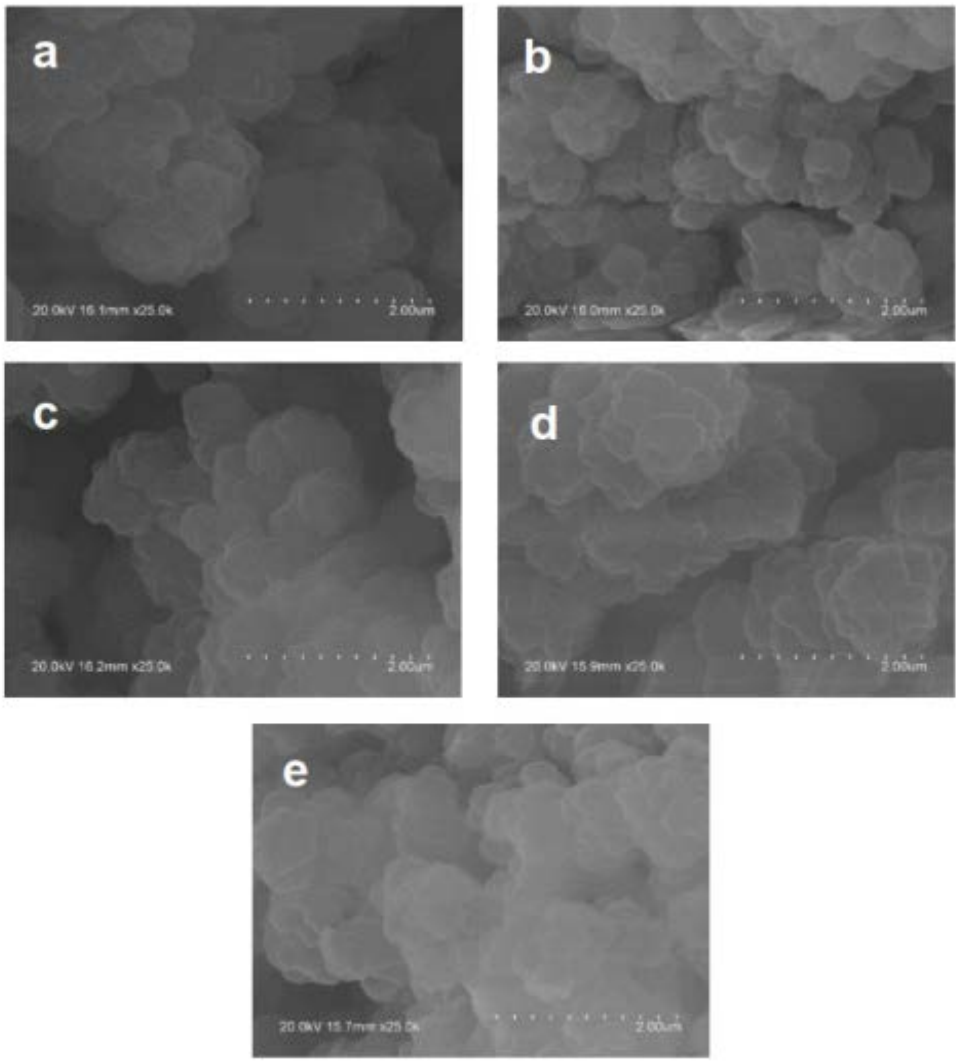

Figure 8. SEM images of monoliths with 2% VMNP obtained at constant resonance frequency (5.5 kHz) and different OMF generation times: (**a**) 1 min, (**b**) 5 min, (**c**) 10 min, (**d**) 20 min and (**e**) 60 min. Images obtained at 20 kV and x25 k magnification.

Based on the reported results, it is established that, in the separation of the toluene-ethylbenzene pair using a polymeric monolithic column with 2% VMNP in the absence of magnetic field, the column resolution is 1.02. While the separation of this ABS pair using a polymeric monolithic column with 2% NPVMV in the presence of magnetic field, under conditions of 5.5 kHz and 10 min exposure in OMF, the Rs increases to 1.35. This chromatographic parameter was quantified based on the literature of Roig[28] and analyzed according to the work of Bose[29]. The resolution data of the other pairs of peaks are shown in **Table 4**, where it can be evidenced that the variables used in this methodology allowed improving the resolution in the chromatographic column.

In order to clarify the influence of exposure time on chromatographic behavior, the morphology of the columns was again studied by SEM (**Figure 8**). However, as was the case with the influence of OMF frequency variation, no appreciable morphological changes in microglobule size were observed with increasing exposure time. According to Jiles and Atherton, excess magnetic field exposure time can generate hysteresis in ferromagnetic materials[30].

Ultimately, in order to establish reproducibility, five of the columns in the absence of OMF were used for chromatographic characterization. Then, to analyze the resonance frequency, four columns were used for each frequency, whereby a value of 5.5 kHz was determined for the best chromatographic separation. Finally, based on this last factor, four monolithic columns were used for each OMF

exposure time. In this way, retention time, separation factor and column resolution were evaluated, with an optimum value of 1.35. These results are close to those reported by Carrasco-Correa *et al.* and Dadoo *et al.*[15,31].

4. Conclusions

The influence of the application of OMF on methacrylate monoliths containing VMNP and the effects on their chromatographic and morphological properties were studied. The application of increasing OMF frequencies resulted in an increase in chromatographic retention. Similarly, the influence of OMF exposure time at a given frequency also resulted in changes in chromatographic retention, but no morphological modifications were evident.

The experimental conditions for the preparation of the monolithic columns and the chromatographic conditions for the analysis were carefully optimized. Thus, the best ABS separation was established at 5.5 kHz and 10 min exposure in the OMF. The application of this factor resulted in an increase in column resolution from 1.02 to 1.35. This translates into a better separation of the analyte components.

These results make this a novel work for the development of miniaturized systems of analysis and future investigations with the use of other test solutes for the evaluation of changes in selectivity, applying different OMF parameters or in the determination of the surface area of monoliths with VMNP subjected to different frequencies and exposure times of OMF.

Conflict of interest

The authors declared no conflict of interest.

References

1. Lynch KB, Ren J, Beckner MA, *et al*. Monolith columns for liquid chromatographic separations of intact proteins: A review of recent advances and applications. Analytica Chimica Acta 2019; 1046: 48–68.
2. Dores-Sousa JL, Fernández-Pumarega A, De Vos J, *et al*. Guidelines for tuning the macropore structure of monolithic columns for high-performance liquid chromatography. Journal of Separation Science 2019; 42(2): 522–533.
3. Liu L, Yang C, Yan X. Methacrylate-bonded covalent-organic framework monolithic columns for high performance liquid chromatography. Journal of Chromatography A 2017; 1479: 137–144.
4. Wang R, Li W, Chen Z. Solid phase microextraction with poly (deep eutectic solvent) monolithic column online coupled to HPLC for determination of non-steroidal anti-inflammatory drugs. Analytica Chimica Acta 2018; 1018: 111–118.
5. Sharma G, Tara A, Sharma VD. Advances in monolithic silica columns for high-performance liquid chromatography. Journal of Analytical Science and Technology 2017; 8(1): 1–11.
6. Kartsova LA, Bessonova EA, Somova VD. Hydrophilic interaction chromatography. Journal of Analytical Chemistry 2019; 74(5): 415–424.
7. Buszewski B, Szumski M. Study of bed homogenity of methacrylate-based monolithic columns for micro-HPLC and CEC. Chromatographia 2004; 60(1): S261–S267.
8. Svec F, Lv Y. Advances and recent trends in the field of monolithic columns for chromatography. Analytical Chemistry 2015; 87(1): 250–273.
9. Poupart R, Grande D, Carbonnier B, *et al*. Porous polymers and metallic nanoparticles: A hybrid wedding as a robust method toward efficient supported catalytic systems. Progress in Polymer Science 2019; 96: 21–42.
10. Li Z, Rodriguez E, Azaria S, *et al*. Affinity monolith chromatography: A review of general principles and applications. Electrophoresis 2017; 38(22–23): 2837–2850.
11. Gama MR, Rocha FRP, Bottoli CBG. Monoliths: synthetic routes, functionalization and innovative analytical applications. TrAC Trends in Analytical Chemistry 2019; 115: 39–51.
12. Terborg L, Masini JC, Lin M, *et al*. Porous polymer monolithic columns with gold nanoparticles as an intermediate ligand for the separation of proteins in reverse phase-ion exchange mixed mode. Journal of Advanced Research 2015; 6(3): 441–448.
13. Aqel A. Using of nanomaterials to enhance the separation efficiency of monolithic columns. Nanomaterials in Chromatography. Elsevier; 2018. p. 299–322.
14. Soriano ML, Zougagh M, Valcárcel M, *et al*. Analytical nanoscience and nanotechnology: Where we are and where we are heading. Talanta 2018; 177: 104–121.
15. Carrasco-Correa EJ, Ramis-Ramos G, Herrero-Martínez JM. Hybrid methacrylate monolithic columns containing magnetic nanoparticles for capillary electrochromatography. Journal of Chromatography A 2015; 1385: 77–84.
16. Barbosa-Canovas G. Food Engineering-Volume III. Washington: EOLSS Publications; 2009.
17. Aguilera-Díaz JD, Parra-Pérez A. Design and construction of a magnetic field generator with intensity,

direction and frequency control (in Spanish) [Undergraduate thesis]. Bogotá: Universidad Santo Tomas de Aquino; 2015.
18. Prieto A, Pereda JA, González O. Opencourseware electricity and magnetism [Internet]. University of Cantabria; 2010. Available from: https://ocw.unican.es/course/view.php?id=197.
19. Tipler PA, Mosca G. Electricity and magnetism. In: Física para la ciencia y la tecnología. Barcelona-Bogotá: Reverté; 2005. p. 878–897.
20. Saien J, Bamdadi H, Daliri S. Liquid-liquid extraction intensification with magnetite nanofluid single drops under oscillating magnetic field. Journal of Industrial and Engineering Chemistry 2015; 21: 1152–1159.
21. Jiménez IR, Gorbeña JCR, Félix ST. [Influence of variable sine wave magnetic field of (22–52) khz and 100 milligauss magnetic induction, on the growth of *Lactobacillus plantarum* used as a probiotic in food (in Spanish). Biotempo 2017; 14(1): 49–55.
22. Petro M, Svec F, Fréchet JMJ. Molded continuous poly (styrene-co-divinylbenzene) rod as a separation medium for the very fast separation of polymers Comparison of the chromatographic properties of the monolithic rod with columns packed with porous and non-porous beads in high-performance liquid chromatography of polystyrenes. Journal of Chromatography A 1996; 752(1–2): 59–66.
23. Yang C, Wang G, Lu Z, *et al*. Effect of ultrasonic treatment on dispersibility of Fe_3O_4 nanoparticles and synthesis of multi-core Fe_3O_4/SiO_2 core/shell nanoparticles. Journal of Materials Chemistry 2005; 15(39): 4252–4257.
24. Yu Q, Dave RN, Zhu C, *et al*. Enhanced fluidization of nanoparticles in an oscillating magnetic field. AIChE Journal 2005; 51(7): 1971–1979.
25. Van Ommen JR, Valverde JM, Pfeffer R. Fluidization of nanopowders: A review. Journal of Nanoparticle Research 2012; 14(3): 1–29.
26. Pantoja JMM. Microwave engineering: experimental techniques (in Spanish). Pearson Educación; 2002.
27. Rios A, Zougagh M. Recent advances in magnetic nanomaterials for improving analytical processes. TrAC Trends in Analytical Chemistry 2016; 84: 72–83.
28. Roig C. Validation of a high resolution liquid chromatography method (HPLC) for the determination of ivabradine tablets. Mem. Instituto de Investig. en Ciencias de la Salud 2012: 63–70.
29. Bose A. HPLC calibration process parameters in terms of system suitability test. Austin Chromatogr 2014; 1(2): 1–4.
30. Jiles DC, Atherton DL. Theory of ferromagnetic hysteresis. Journal of Applied Physics 1984; 55(6): 2115–2120.
31. Dadoo R, Zare RN, Yan C, *et al*. Advances in capillary electrochromatography: Rapid and high-efficiency separations of PAHs. Analytical Chemistry 1998; 70(22): 4787–4792.